2016

Novel Reduced GWP Refrigerant Compositions To Replace R-134a in Stationary Air-conditioning and Refrigeration

Laurent Abbas
ARKEMA Inc, United States of America, laurent.abbas@arkema.com

Sarah Kim
ARKEMA Inc, United States of America, sarah.kim@arkema.com

Kenneth Schultz
Trane Technologies, United States of America, kschultz@tranetechnologies.com

Abbas, Laurent; Kim, Sarah; and Schultz, Kenneth, "Novel Reduced GWP Refrigerant Compositions To Replace R-134a in Stationary Air-conditioning and Refrigeration" (2016). *International Refrigeration and Air Conditioning Conference.* Paper 1707.
https://docs.lib.purdue.edu/iracc/1707

Novel Reduced GWP Refrigerant Compositions to replace R-134a in Stationary Air-conditioning and Refrigeration

Laurent ABBAS[1]*, Sarah KIM[1], Kenneth SCHULTZ[2]

[1]Arkema Inc, Fluorochemicals,
King of Prussia, PA, USA
Tel. 610-878-6238, Fax. 610-878-, laurent.abbas@arkema.com

[2]Ingersoll Rand, Technology Validation Team,
Lacrosse, WI, USA
Tel. 608-787-3735, Fax. 608-787-2669, kschultz@trane.com

* Corresponding Author

ABSTRACT

Hydrofluorocarbons (HFCs) have replaced chlorofluorocarbons (CFCs) and hydrochlorofluorocarbons (HCFCs) as non-ozone depleting fluids in many applications, including as refrigerants, solvents, aerosols, and blowing agents for insulating foams. However, some HFCs have relatively high Global Warming Potential (GWP) and are coming under closer scrutiny due to the increasing concern over global climate change. The focus now is on the search for the next generation of environmentally sustainable working fluids with negligible direct environmental impact in terms of both ozone depletion and global warming potential.

Development of low-GWP options should be balanced with respect to safety, performance, ease of use, and energy efficiency. Indeed, greenhouse gas emissions come not only from direct emissions but also largely from indirect sources based on energy consumption. It is therefore important that energy efficiency remain a primary consideration when implementing low-GWP solutions, as replacing a high-GWP fluid with a lower GWP, but less efficient option may actually increase greenhouse gas emissions, thereby degrading the overall Life Cycle Climate Performance (LCCP).

This paper introduces ARM-42, a near-azeotropic, low-GWP refrigerant to replace R-134a. The thermodynamic properties of ARM-42 make it a very close match to R-134a from both a performance, capacity, and efficiency as well as operating pressures standpoint. Single Tube Heat Transfer testing confirmed ARM-42's potential to replace R-134a.

1. INTRODUCTION

In line with the world wide effort to reduce the usage of high Global Warming Potential (GWP), the momentum to replace high direct GWP refrigerants is increasing, especially in Europe with the phase down of CO2 equivalent quota and in US with the EPA SNAP delisting program. To that purpose, hydrofluoroolefins (HFOs) offer many of the benefits of HFCs but with the added benefit of very low GWP. This comes from the extremely short atmospheric lifetimes of these compounds resulting from their olefinic structure. As such, HFOs are attractive next-generation solutions potentially offering excellent environmental profile and performance.

One of the most widely used HFC refrigerant for medium temperature application, R-134a, has a relatively high GWP (1300, Stocker et al. 2013) and its replacement has generated a lot of interest. R-1234yf has been proven to be a good replacement for R-134a in medium temperature applications including mobile air-conditioning (SAE, 2009). R-1234ze has been proposed as a replacement of R-134a for positive and centrifugal chillers (Spatz, 2012). In a chiller application, the use of R-1234yf itself results in more than 6% lower efficiency versus R-134a. The use of R-1234ze in the same condition results in over 25% loss in capacity (Schultz et al, 2014).

In this paper ARM-42, a novel, low GWP refrigerant to replace R-134a is presented. Thermodynamic and heat transfer properties are discussed along with the physical and environmental properties of the refrigerant.

2. REFRIGERANT PROPERTIES

ARM-42 is a near-azeotropic blend of R-1234yf (2,3,3,3-tetrafluoropropene), R-134a (1,1,1,2-tetrafluoroethane), and R-152a (1,1-difluoroethane) (77.5%wt/8.5%wt/14.0%wt).

2.1 Compatibility and Stability

HFC-134a is used with polyol ester (POE) type lubricating oils. The miscibility of ARM-42 with typical POE lubricants was tested over a wide range of concentrations and temperatures that covers the operating ranges typically encountered in commercial refrigeration and air-conditioning. ARM-42 was found to be comparable to that of HFC-134a.

The stability of ARM-42 in the presence of materials that it would likely encounter in practical use was evaluated in sealed tube tests according to the ASHRAE Standard 97-2007. At test conditions, ARM-42 and ARM-42/POE blends in the presence of steel, copper, and aluminum showed thermal stability comparable to that of HFC-134a.

2.2 Flammability

ARM-42 has been found to be flammable per testing done according to ASHRAE Standard 34-2013. The burning velocity has been measured at <10 cm/s and ARM-42 would therefore be classified as an A2L. The flammability properties of ARM-42 are presented in Table 1.

Table 1: Flammability properties of ARM-42.

LFL (%v/v) @23°C	4.5
Burning velocity (cm/s) @23°C	6.0

2.3 Thermodynamic Properties

2.3.1 Blend properties: The thermodynamic properties of ARM-42 are presented in Table 2 and compared to R-134a and other slightly flammable R-134a replacements.

Table 2: Thermodynamic properties of R-134a and R-134a replacement candidates

	R-134a	ARM-42	R-1234yf	R-1234ze(E)
GWP_{100}	1300	131	<1	<1
Flammability	A1	A2L*	A2L	A2L
Bubble point (°C) at 1atm**	-26.1	-29.4	-29.5	-19.0
Dew point (°C) at 1atm**	-26.1	-29.3	-29.5	-19.0
Critical Temperature (°C)**	101.1	96.8	94.7	109.4
Critical Pressure (MPa)**	4.1	3.6	3.4	3.6
Liquid Density at 25°C (kg/m^3)**	1206.7	1069.2	1091.9	1163.1
Vapor Density at 25°C (kg/m^3)**	32.4	34.5	37.9	26.3

** Anticipated classification*
*** R-134a, R-1234yf and R-1234ze properties were obtained using REFPROP (Lemmon et al, 2013). ARM-42 properties were obtained through proprietary measurements and models.*

The vapor pressure of ARM-42 is very close to R-134a for a wide range of temperature as shown in Figure 1. Minor differences can only be observed for temperatures above 60°C.

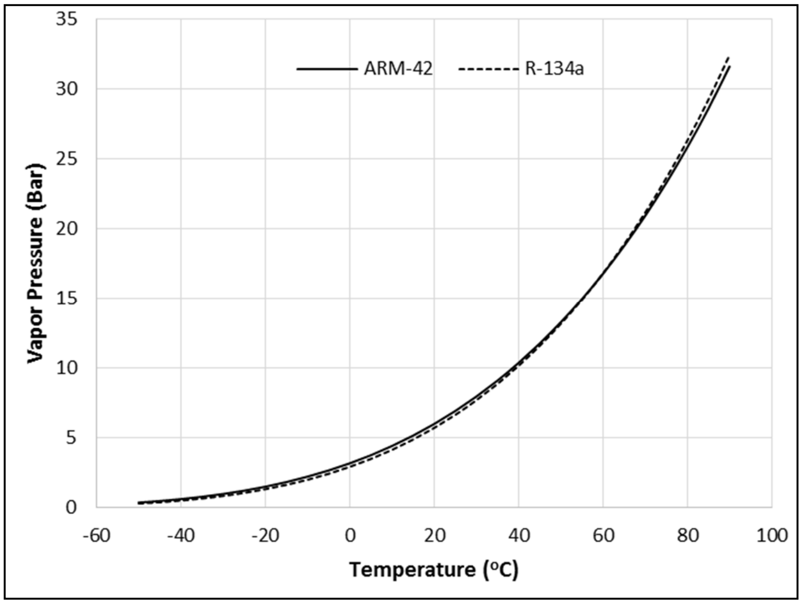

Figure 1: Vapor Pressure of ARM-42

ARM-42 is a near-azeotropic refrigerant with almost no glide. The maximum glide value of about 0.06°C is obtained at 0.1 MPa where the saturation temperature is -29.6°C. The evolution of the glide as a function of the pressure is shown in Figure 2.

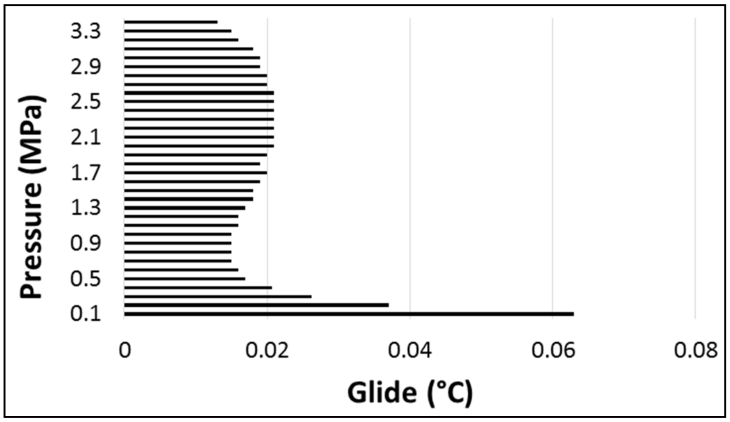

Figure 2: Glide of ARM-42

<u>2.3.2 Simple Thermodynamic calculation:</u> The performance of ARM-42 was calculated for a simple cycle for the conditions presented in table 3 below

Table 3: Simple Cycle Conditions

Evaporation Temperature (°C)	4.4
Evaporator Superheat (°C)	0
Condensation Temperature (°C)	37.8
Condenser Subcooling (°C)	5.6
Compressor Efficiency	0.7

A simple thermodynamic model is used here to compare the various refrigerants to each other. The model does not account for heat transfer, pressure drop, and compressor effects and compares only the thermodynamic characteristics of the various fluids. The model assumes the same condenser and evaporator saturation temperatures, evaporator leaving superheat, condenser leaving subcooling, and compressor isentropic efficiency for all refrigerants.

The P,H and T,S diagram of ARM-42 are presented Figure 3 and Figure 4 and compared to R-134a and R-1234ze(E) (trans-1,3,3,3-tetrafluoropropene) under the same conditions. The width of the ARM-42 dome, representing the latent heat of vaporization, is slightly narrower than for R-134a. R-1234ze has a similar dome width to that of ARM-42 but operating pressures are significantly lower.

Figure 5 shows the performance of ARM-42 and R-1234ze(E) at the same operating conditions compared to R-134a. For these temperatures, ARM-42 delivers similar cooling capacity to R-134a and slightly reduced efficiency by 2%. At the same conditions, R-1234ze exhibited a very close match to R-134a in term of efficiency but showed a significantly reduced cooling capacity. The 25% loss of capacity would have to be compensated by a larger volumetric displacement compressor. Modifications of the size of the heat exchangers may also be needed due to lower vapor density.

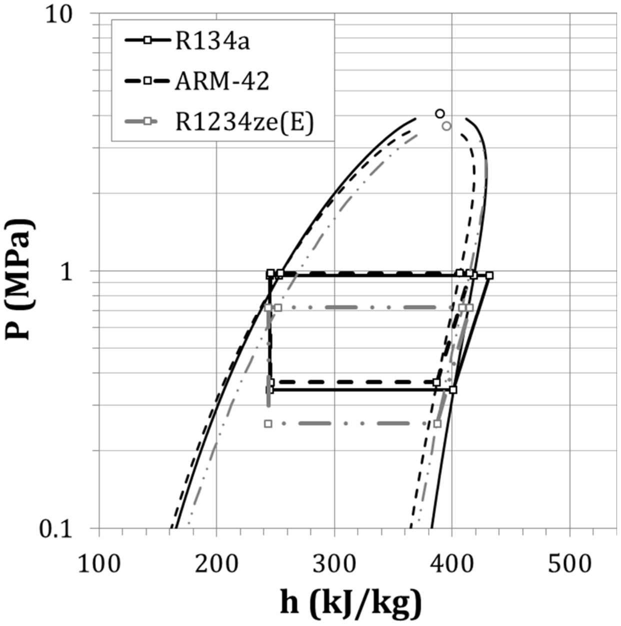

Figure 3:. Pressure-enthalpy chart for R-134a, ARM-42 and R-1234ze

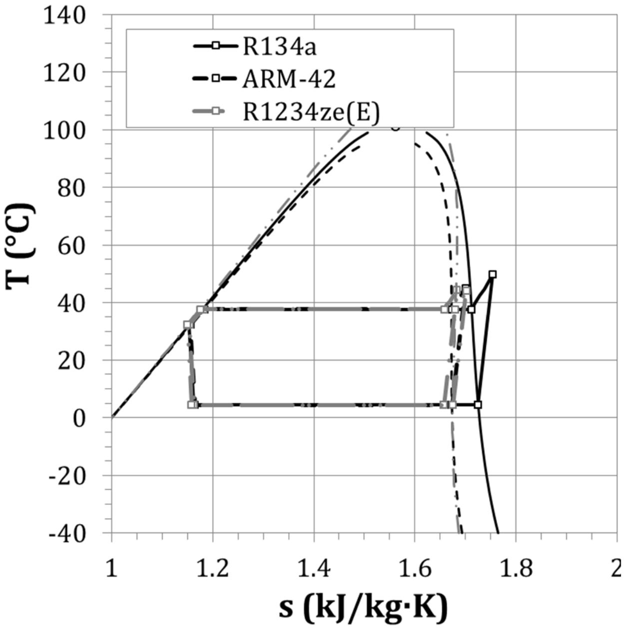

Figure 4: Temperature-entropy chart for R-134a, ARM-42 and R-1234ze

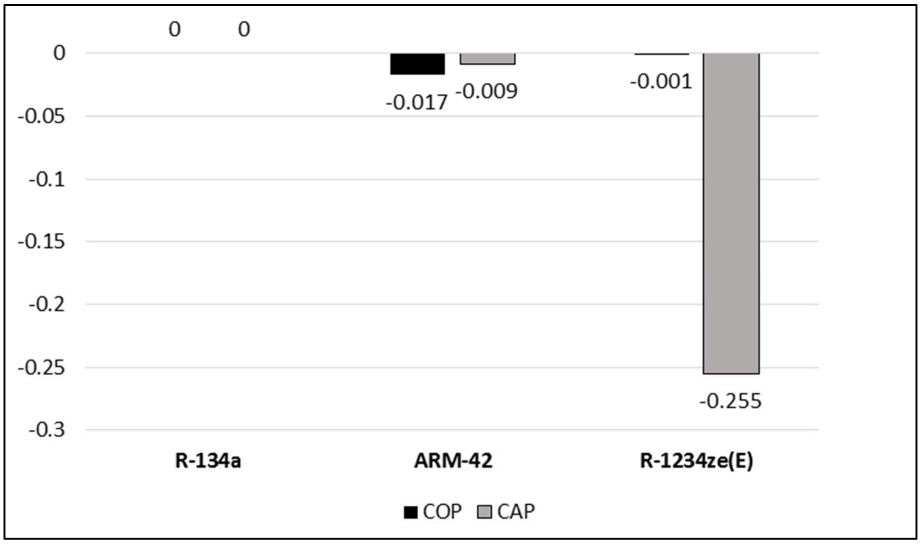

Figure 5: Performance of ARM-42 and 1234ze(E) relative to R-134a in a simple thermodynamic cycle

3. HEAT TRANSFER TESTING

3.1 Description of the tests

Single Tube Heat Transfer was performed at the Ingersoll Rand testing facility in La Crosse, WI. The test set-up consisted in two shells of 6” Schedule 40 pipe. The pressure is the same in both shells (thermosiphon effect). The chilled water was supplied to the condenser tube and warm water was supplied to the evaporator tube.

Refrigerant-side measurements in condenser consist of:

- Two pressure transducers attached to the shell.
- Two RTDs inserted into shell from top with ~7.6 cm of insertion length (to within 3 mm of the top of the center tube). Although well insulated, the RTDs act as dew point sensors when the condensing saturation temperature is higher than the ambient temperature in the facility.

Refrigerant-side measurements in evaporator consist of:

- Two pressure transducers attached to the shell.
- Two RTDs inserted into shell from bottom with ~5 cm of insertion length (to within 12 mm of the bottom of the center tube). We assume these RTDs give an accurate measure of the (saturated) refrigerant pool temperature at the depth of the tube.

Heat transfer coefficients are calculated as follows:

- Heat transfer rate is determined from water-side measures of flow rate and inlet and outlet temperatures and pressures:

$$\dot{Q} = \dot{m} \cdot \left(h(T_{in}, P_{in}) - h(T_{out}, P_{out}) \right) \tag{1}$$

- The overall heat transfer coefficient, U_o, is calculated as follows

$$U_o = \frac{\dot{Q}/A_o}{LMTD} \qquad LMTD_{Cond} = \frac{T_{out} - T_{in}}{ln\left(\frac{T_{sat} - T_{out}}{T_{sat} - T_{in}}\right)} \qquad LMTD_{Evap} = \frac{T_{in} - T_{out}}{ln\left(\frac{T_{sat} - T_{in}}{T_{sat} - T_{out}}\right)} \tag{2}$$

- The shell-side or refrigerant-side heat transfer coefficient , h_o, is then determined as follows:

$$\frac{1}{h_o} = \frac{1}{U_o} - R_{wall} - \beta_2 FF - \frac{\beta_1}{h_i} \tag{3}$$

where : R_{wall} is the thermal resistance of the tube wall
FF is the thermal resistance due to fouling, typically assumed to be zero.
h_i is the tube inside heat transfer coefficient, typically supplied by the tube vendor

3.2 Condensing results

Based on using the average dew point temperature reported by the two RTDs inserted into the condenser shell, the condensing coefficients for ARM-42 are presented Figure 6.

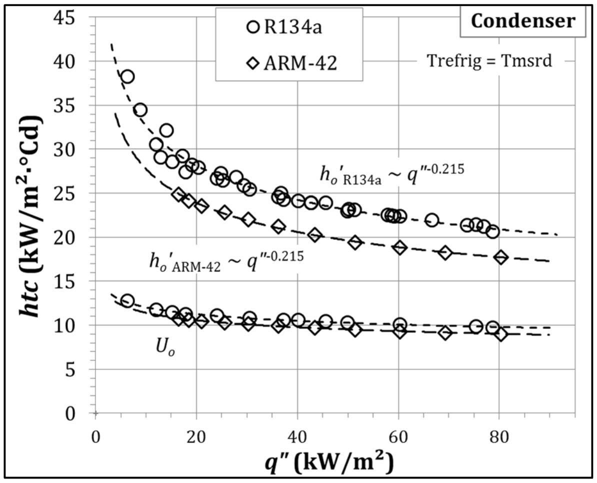

Figure 6: Heat transfer measurements for R-134a, ARM-42 in the condenser

The condensing heat transfer coefficient with ARM-42 is 15% lower than with R-134a. The exponents on the h_o' least squares fit power law equations are identical to three digits for both R-134a and ARM-42. Schultz (2014) reported much lower performance of ARM-42 in a chiller shell-and-tube water-cooled condenser. In that test, the refrigerant saturation temperature was inferred from the measured shell pressure through the saturated pressure-temperature relationship known at that time. Recent review of that data indicates that the low values of condensing heat transfer coefficient are likely due to the inaccuracy of the saturation curve available at that time at typical condenser operating conditions (~38°C saturation temperature). The heat transfer coefficients in Figure 6 were computed from the direct measurements of saturation temperature to eliminate any uncertainty in the saturation pressure-temperature relationships. However, the accuracy of the temperature measurements here is supported by close agreement (<0.1K) with the temperatures returned by the current saturation equations for both R-134a and ARM-42 from the measured shell pressures.

3.3 Evaporating results

The pool boiling heat transfer coefficients presented here are based on the direct pool temperature measurements to eliminate any uncertainty in the saturation curves as discussed above. Similar to the condensing results, the average of the two probe measurements was used. Results are shown in Figure 7.

The overall evaporator heat transfer coefficient is 2% to 4% lower with ARM-42 than with R134a. The refrigerant-side pool boiling heat transfer coefficient with ARM-42 is approximately 10%-15% lower than with R134a. This is consistent with the results from a chiller test (Schultz, 2014), where the accuracy of the original saturation curve was better at typical evaporator operating conditions (~4°C saturation temperature).

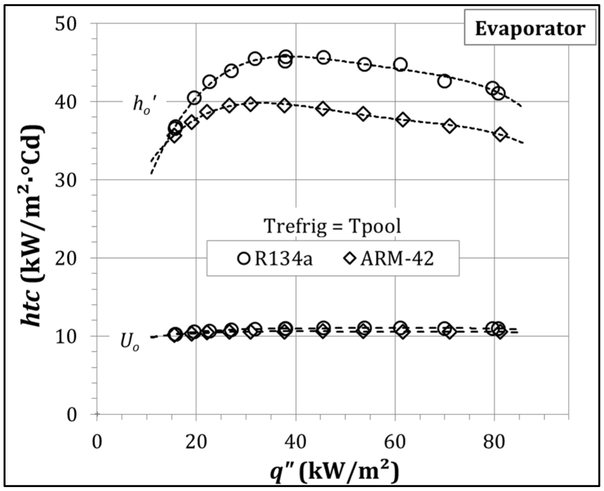

Figure 7: Heat transfer measurements for R-134a, ARM-42 in the evaporator

4. CONCLUSIONS

ARM-42 is a near-azeotropic blend of HFO-1234yf, HFC-134a and HFC-152a (77.5%wt/8.5%wt/14%wt) with a 100 year GWP of less than 150. Thermodynamic properties of ARM-42 makes it a very close match to R-134a from both performance, capacity and efficiency, and operating pressures. Heat transfer testing on ARM-42 has shown a reduction of about 15% in both condensing and evaporating heat transfer coefficients relative to R-134a that may suggest a modification of the tube surfaces is needed to obtain optimal performance with ARM-42. This work is however not completed and performance of full chiller testing with ARM-42 will be discussed in the near future.

NOMENCLATURE

$\dot{Q}$	Heat transfer rate	(W)
$\dot{m}$	Water-side flow rate	(kg/s)
$h(T_{in}, P_{in})$	Water-side Inlet Enthalpy	(J/kg)
$h(T_{out}, P_{out})$	Water-side Outlet Enthalpy	(J/kg)
U_o	Overall heat transfer coefficient	(W/m^2K)
A_o	Heat exchanger area	(m^2)
$LMTD$	Log Mean Temperature difference	(K)
$LMTD_{evap}$	Log Mean Temperature difference evaporator	(K)
$LMTD_{cond}$	Log Mean Temperature difference condenser	(K)
T_{sat}	Shell-side Temperature	(K)
T_{im}	Water-side Inlet Temperature	(K)
T_{out}	Water-side Outlet Temperature	(K)
h_o	Shell-side heat transfer coefficient	(J/kg)
R_{wall}	Thermal resistance of the tube wall	(m^2K/W)
FF	Thermal resistance due to fouling	(m^2K/W)
h_i	Tube-side heat transfer coefficient	(W/m^2K)

REFERENCES

ASHRAE Standard 34-2013, “Designation and Safety Classification of Refrigerants”, 2013

ASHRAE Standard 97-2007, “Sealed Glass Tube Method to Test the Chemical Stability for Materials for Use within Refrigeration Systems:, 2007

Lemmon, Eric W.; Huber Marcia L.; McLinden Mark O., NIST Standard Reference Database 23, “Reference Fluid Thermodynamic and Transport Properties-REFPROP”, Version 9.1, 2013

SAE CRP 1234. “Industry Evaluation of Low Global Warming Potential Refrigerant”, 2009

Schultz K. (2014). Performance of R134a Alternative Lower GWP Refrigerants in a Water-Cooled Screw Chiller, *Conference Paper NY-14-C065, ASHRAE Papers CD: 2014 ASHRAE* Winter Conference, New York, NY

Spatz, Mark W.; Sethi, Ankit; and Yana Motta, Samuel F., “Latest Developments of Low Global Warming Refrigerants for Chiller” (2012). *International Refrigeration and Air Conditioning Conference*. Paper 1352